Inorg. Chem. **1993,** *32,* 2815–2820

Stereochemistry of Thiocyanate Photoanation in *trans*-$CrCl(NH_3)(1,3\text{-diaminopropane})_2^{2+}$

A. D. Kirk*

Department of Chemistry, University of Victoria, P.O. Box 3055, Victoria, BC, Canada V8W 3P6

C. Namasivayam

Department of Chemistry, Bharathiar University, Coimbatore 641046, Tamil Nadu, India

Received January 5, 1993

The compound *trans*-$CrCl(NH_3)(tn)_2^{2+}$ (where tn = 1,3-diaminopropane) has been synthesized, characterized and the structure determined by X-ray single-crystal methods. The crystal is monoclinic, $P2_1/n$ (No. 14), with chemical composition *trans*-$[CrCl(NH_3)(tn)_2]_2(ClO_4)_3(NO_3)\cdot H_2O$, M_r = 883.8, and a = 13.516(1) Å, b = 9.749(2) Å, c = 26.533(3) Å, β = 93.02(1)°, V_{cell} = 3491.3 Å^3, and Z = 4 (asymmetric unit was $Cr_2Cl_2N_{11}C_{12}H_{48}O_{16}$). In acidic aqueous solution at room temperature, the compound loses chloride at a slow rate (rate constant $<5 \times 10^{-7}$ s^{-1} at 28 °C), but photolysis leads to aquation of ammonia with a wavelength independent quantum yield of 0.33 ± 0.01 to give *cis*-$CrCl(H_2O)(tn)_2^{2+}$ as the only observable product, the total chloride yield having an upper limit of 0.003. When photolyzed in the presence of thiocyanate ion, *cis*-$CrCl(NCS)(tn)_2^+$ is produced in competition with the aquation, and the quantum yield of ammonia loss remains unchanged over the range 0–3 M NCS^-. These results show that photoanation competes with photoaquation and that both processes occur with entry of the substituting nucleophile trans to the displaced ammonia ligand. Chromatographic studies of the products of thermal and photoaquation followed by thermal thiocyanate anation of *trans*- and *cis*-$CrCl_2(tn)_2^+$ were used to identify the photoproduct. This work additionally revealed that, thermally, direct displacement of chloride by thiocyanate can occur in competition with anation, particularly for *cis*-$CrCl(H_2O)(tn)_2^{2+}$.

Introduction

Irradiation of photoactive Cr(III) complexes in their ligand field absorption bands in aqueous solution generally leads to ligand replacement by solvent.[1,2] The characteristics of the process are now fairly well-established, and the most notable feature is that, with a few exceptions, the substituting ligand enters the coordination sphere trans to the leaving ligand, corresponding to a photochemical edge-displacement process.[2,3] The behavior is striking when contrasted with the stereoretentive character of the thermal substitution processes of the same complexes in aqueous media. More dramatic still, there is strong evidence that incorporation of constraining ligands that prevent this edge-displacement mechanism can render the complexes essentially photoinert.[4–7] Thus, for such systems, the stereochemical change seems to be a requirement of photoaquation.

All of the examples that have been well characterized have been photoaquations, however, and it is rather a moot point whether the same features should be expected in other solvent systems or for other types of substitutions. To underline why this question should be raised, consider that the stereoretentive nature of thermal substitutions in aqueous solutions does not carry over to the analogous reactions in dmso or liquid ammonia.[8,9] Similarly, in Co(III) substitutional chemistry, there have been reported differences in entering ligand competition ratios depending on whether the substituting ligand is charged or neutral.[10] This suggests the possibility of analogous effects on the stereochemistry of photosubstitution.

With this as background we have sought to investigate other situations where stereochemical change can be investigated. Krause and Wasgestian[11,12] have shown that, in concentrated solutions of appropriate anions, photoanation occurs in competition with photoaquation from both quartet and doublet states of hexammine Cr(III) systems. The present study has been undertaken to explore whether in these and similar systems, photoanation also occurs with stereochemical change. To this end we have synthesized and characterized a new compound, *trans*-$CrCl(NH_3)(tn)_2^{2+}$. Since absolute proof of the geometric configuration of the material is essential to our purposes and is difficult to establish unambiguously by spectroscopic methods when only a single isomer is available, an X-ray single-crystal structure of the compound has been determined. These results and a study of *trans*-$CrCl(NH_3)(tn)_2^{2+}$ photoaquation and thiocyanate photoanation are reported here.

Experimental Section

Synthesis. *cis*-[13] and *trans*-$[CrCl_2(tn)_2](ClO_4)$,[14] *cis*-$[Cr(NH_3)_2(tn)_2]Cl_3$,[13] and $[Cr(tn)_3](ClO_4)_3$[13] were prepared according to literature methods. *Caution*! All these perchlorate salts are potentially explosive.

trans-$[CrCl(NH_3)(tn)_2](ClO_4)_2$ was synthesized from *trans*-$[CrCl_2(tn)_2]ClO_4$. A 4.5-g (12-mmol) sample of *trans*-$[CrCl_2(tn)_2]ClO_4$ was transferred to a 50-mL Carius tube, and about 20 mL of anhydrous ammonia was condensed onto it by using dry ice/ethanol cooling under vacuum. After being sealed, the tube was allowed to warm to room temperature for about 15 min, during which time the green solution completely changed to red. The reaction mixture was cooled in dry ice

---

* Author to whom correspondence should be addressed.

(1) Zinato, E. In *Concepts of Inorganic Photochemistry*; Adamson, A. W., Fleischauer, P. (Eds.), Wiley, New York, **1975**, Chapter 4.
(2) Kirk, A. D. *Coord. Chem. Rev.* **1981**, *39*, 225.
(3) Vanquickenborne, L. G.; Ceulemans, A. *Coord. Chem. Rev.* **1983**, *48*, 157.
(4) Kutal, C.; Adamson, A. W. *Inorg. Chem.* **1973**, *12*, 1990.
(5) Kane-Maguire, N. A. P.; Wallace, K. C.; Miller, D. B. *Inorg. Chem.* **1985**, *24*, 597.
(6) Kane-Maguire, N. A. P.; Crippen, W. S.; Miller, P. K. *Inorg. Chem.* **1983**, *22*, 696.
(7) Kirk, A. D. *Comm. Inorg., Chem.* **1993**, *14*, 89.
(8) Palmer, D. A.; Watts, D. W. *Aust. J. Chem.* **1968**, *21*, 2895.
(9) Wong, C. F. C.; Kirk, A. D. *Inorg. Chem.* **1976**, *15*, 1519.
(10) Viaene, L.; D'Olieschlager, J.; De Jaegere, S. *Bull. Soc. Chim. Belg.* **1976**, *85*, 89.
(11) Krause, H. H.; Wasgestian, F. *Inorg. Chim. Acta* **1981**, *49*, 231.
(12) Krause, H. H.; Wasgestian, F. *Inorg. Chim. Acta* **1983**, *76*, L295.
(13) Pedersen, E. *Acta Chim. Scand.* **1970**, *24*, 3362.
(14) House, D. A. *Inorg. Nucl. Chem. Lett.* **1970**, *6*, 741.3.

0020-1669/93/1332-2815$04.00/0

and the tube opened. The ammonia was allowed to evaporate, with the last amounts requiring evacuation (yield: 3.7 g; 8.2 mmol; 68%).

The crude complex was recrystallized by dissolving it in a minimum volume of 1 M $HClO_4$ and filtration of any insoluble residue of starting material. To the filtrate, 10 mL of 60% perchloric acid was added dropwise with stirring and the solution was kept in the refrigerator for 30 min. The crystals that formed were washed with 2-propanol and ether and dried in vacuum.

Analysis. Microanalysis was by Canadian Microanalytical Services except for Cr which was by 50% nitric acid decomposition followed by oxidation with alkaline H_2O_2.[15] The chromate ion formed was then determined at 372 nm ($\epsilon = 4.82 \times 10^3$ L mol^{-1} cm^{-1}).

Results. Calcd (found) for *trans*-$[CrCl(NH_3)(tn)_2](ClO_4)_2$: Cr, 11.52 (11.35); C, 15.95 (16.10); H, 5.10 (5.20); N, 15.20 (15.48); Cl, 23.58 (24.68).

UV–Vis Data. UV–vis (nm (ϵ, L mol^{-1} cm^{-1})) spectral measurements were made with a Pye-Unicam SP8-400 spectrophotometer: λ_{max}, 376 (53.5), 524 (36.2); sh, 476 (28.3); λ_{min}, 424 (17.7).

X-ray Crystal Structure. To avoid the disorder problems commonly encountered in perchlorate lattices, single crystals were prepared starting from the perchlorate salt but recrystallizing from acidic nitrate solutions. Good crystals were easily obtained. Analysis and the X-ray studies showed that the red, monoclinic crystals so obtained were not of the dinitrate, but corresponded to the composition $[CrCl(NH_3)(tn)_2]_2(ClO_4)_3(NO_3)\cdot H_2O$.

X-ray Data Collection. Symmetry and approximate unit cell dimensions for the crystal were established by preliminary photographic work with Weissenberg and precession cameras using Cu K α radiation. Density measurement was by flotation. Using a Picker four-circle diffractometer, 25 pairs of centering measurements were used in a least squares procedure to refine the unit cell.

The Picker system used a $\theta/2\theta$ scan with 160 steps of 0.010 in 2θ, with counting for 0.25 s at each step. Background measurements were for 20 s at the beginning and end of each scan. Each batch of 50 reflections was preceded by the measurement of three standards, and after the application of Lorentz and polarization factors, each batch was scaled to keep the sum of the standards constant. Measurements were in the 2θ range 22–43°, with $h = -14$ to $+14$, $k = 0$–10, and $l = 0$–29. Absorption corrections were applied by a numerical integration using a Gaussian grid and using the crystal shape defined by perpendicular distances to crystal faces from a central origin. There was significant decomposition of the crystal during the diffraction measurements, and this limited the extent of data collection and the precision of the final structure.

Structure Solution and Refinement. The structure was found and refined using SHELX-76,[16] and illustrations were generated using ORTEP.[17] The atomic scattering values were for neutral atoms, with corrections for anomalous dispersion.[18] The structure was solved by direct methods, developed by standard Fourier synthesis procedures using difference maps and refined by the method of least squares. Hydrogen atoms were not located. The structure refined to final R and R_w values of 0.122 and 0.118, using 3520 independent observed reflections ($I > 4\sigma(I)$) of the 4926 measured.

Chromatographic Analysis. A Varian Model 5000 liquid chromatograph with UV–vis detector and a 25-cm octadecylsilane (10 μm) column was employed. The eluent was 25 mM sodium hexanesulfonate (HSA) plus 25 mM triethylammonium (TEA) ion in 40% methanol/water at pH values of 3.0 and 4.3. Complexes were detected at a wavelength of 240 nm. For the identification of 2+ and 3+ ions, 25 mM sodium butanesulfonate (BSA) plus 25 mM triethylammonium ion in 100% water at pH 3.0 was employed. To indicate where such 3+ ions should elute, authentic samples[19] of $Cr(tn)_3^{3+}$ and *cis*-$Cr(NH_3)_2(tn)_2^{3+}$ were used as chromatographic markers.

Identification and Determination of the Thermal and Photoproducts. This was carried out by HPLC on solutions of known compounds, and similar solutions that had been photolyzed and/or thermolyzed. The method necessitated reliance on chromatographic retention times; these were found to be reproducible within a few percent, sufficient to be sure about peak sequences and identities, as shown later. Unfortunately, the quantities of materials in these peaks are too small (about 50 nmol) for collection and analysis to be feasible at present.

Table I. Selected Crystallographic Data for *trans*-$[CrCl(NH_3)(tn)_2]_2(ClO_4)_3(NO_3)\cdot H_2O$

formula	$C_{12}H_{48}O_{16}N_{11}Cl_5Cr_2$	fw	883.8
space group	$P2_1/n$ (No. 14)	cryst syst	monoclinic
a (Å)	13.516(1)	c (Å)	26.533(3)
b (Å)	9.749(2)	β (deg)	93.02(1)
V (Å^3)	3491.3	Z	4 (8 Cr)
ρ_{meas} (g cm^{-3})	1.66	ρ_{calc} (g cm^{-3})	1.681
diffractometer	Picker 4 circle	radiation, λ (Å)	1.542
μ (cm^{-1})	70.01	temp (K)	293
cryst color	red	size (mm)	0.95 × 0.42 × 0.12
no. of measd reflcns	4926	no. of obsd reflcns	3520
R	0.1216[a]	R_w	0.1184[a]

[a] $\sum w/\Delta^2$; $w = 1/(\sigma^2(F) + 0.001F^2)$; $\Delta = \|F_o| - |F_c\|$. $R = (\sum\Delta/\sum F_o)$; $R_w = (\sum w\Delta^2/\sum sF_o^2)^{1/2}$.

Chloride Analysis. Chloride was estimated semiquantitatively by passing the photolyzed solution (2.5 mL) of the *trans*-$CrCl(NH_3)(tn)_2^{2+}$ through an ion exchange column (Dowex 50W, H^+ form, 6.0 × 0.9 cm) to isolate any free Cl^- ion. The eluent was collected in a test tube and mixed with 1 M $AgNO_3$ solution, and the turbidity observed was compared with the turbidity obtained from water, 5×10^{-5}, 1×10^{-4}, and 5×10^{-4} M NaCl solutions. The turbidity of 5×10^{-5} M Cl^- could be clearly observed in a test tube when viewed at right angles with illumination from a microscope illuminator. This simple procedure was almost as sensitive as the more elaborate and time-consuming concentration cell technique used in earlier work.[20]

Quantum Yield Determinations. Radiation at 360 or 436 nm (Balzers interference filter) from a 1000-W mercury lamp was passed through a 10-cm water filter to remove the IR radiation. Efficiently stirred solutions in 1-cm rectangular cuvettes were thermostated at 28 or 10 °C during irradiation, and the pH was monitored continuously by an Ingold LOT combination electrode interfaced to a PDP-11 computer. By means of additions of standard acid from a 200-μL stepping motor buret, the pH of the solution was maintained constant with periodic recording of acid added. This permitted measurements of the rates of photochemical reactions such as the following, both of which lead to proton uptake.

$$CrCl(NH_3)(tn)_2^{2+} + H_3O^+ \rightarrow CrCl(H_2O)(tn)_2^{2+} + NH_4^+ \quad (1)$$

$$CrCl(NH_3)(tn)_2^{2+} + H^+ + NCS^- \rightarrow CrCl(NCS)(tn)_2^+ + NH_4^+ \quad (2)$$

The advantages of the pH-stat method over the ΔpH method are mentioned in a previous paper.[21] The most important is that maintaining the pH constant eliminates uncertainties that arise in the ΔpH method from partial dissociation of photoproducts to the conjugate base forms.

The light intensity from the lamp was computer-monitored continuously by using the analogue output from an Alphametrics 1200 photometer and silicon diode photodetector calibrated in terms of the ferrioxalate actinometer. Test experiments and results presented here show that the method has a relative standard deviation of better than 3%.

Results

X-ray Crystal Structure. Selected crystallographic parameters, the unit cell positions, selected bond lengths and angles are given in Tables I–III. The Ortep diagram of one of the two, similar, complex ions in the asymmetric unit is shown in Figure 1. The compound has the *trans* configuration. Moreover, the two tn rings are in a chair conformation as is also found[22,23] for close analogues. Finally, the data illustrates the ability of this compound to form mixed perchlorate nitrate salts. Similar behavior has been previously reported[5] for the somewhat similar cyclam analogues. The bond lengths and angles, Table III, have

---

(15) Kirk, A. D.; Namasivayam, C.; Ward, T. *Inorg. Chem.* **1986**, *25*, 2225.

(16) Sheldrick, G. M. SHELX-76, A Computer Program for Crystal Structure Determination. University of Cambridge, England, 1976.

(17) Johnson, C. K. *ORTEP, A Fortran Thermal Ellipsoid Plot Program for Crystal Structure Illustrations*; Report ORNL-3794; Oak Ridge National Laboratory: Oak Ridge, TN, 1965.

(18) Ibers, J. A.; Hamilton, W. C., Eds. *International Tables for X-Ray Crystallography*; Kynoch Press: Birmingham, England, 1974; Vol. 4.

(19) Kirk, A. D.; Ibrahim, A. M. *Inorg. Chem.* **1988**, *27*, 4567.

(20) Wong, C. F. C.; Kirk, A. D. *Can. J. Chem.* **1974**, *52*, 3384.

(21) Kirk, A. D.; Heyd, D. *Inorg. Chem.* **1991**, *30*, 2453.

(22) Vaughn, J. E. *Inorg. Chem.* **1981**, *20*, 2397.

(23) Jurnak, F. A.; Raymond, K. N. *Inorg. Chem.* **1974**, *13*, 2387.

Table II. Fractional Atomic Coordinates and Temperature Parameters[a]

atom	*x/a*	*y/b*	*z/c*	U_{eq} (Å^2)
Cr(1)	34008(13)	12852(20)	7470(7)	270(6)
Cr(1′)	55681(13)	46443(20)	32157(7)	292(6)
Cl(1)	35049(24)	10506(35)	−1175(11)	445(11)
Cl(1′)	40597(23)	53855(35)	34832(13)	469(11)
Cl(2)	83722(26)	3837(40)	36315(13)	526(12)
Cl(3)	−8104(30)	22121(50)	2115(15)	649(15)
Cl(4)	23132(27)	46966(38)	20818(14)	542(13)
N(1)	3299(7)	1462(11)	1527(3)	37(3)
N(2)	2565(7)	−527(11)	740(4)	38(4)
N(3)	4701(7)	170(11)	859(4)	38(4)
N(4)	4283(7)	3031(11)	747(4)	41(4)
N(5)	2088(7)	2450(11)	660(4)	38(3)
C(1)	2872(10)	−1714(14)	1068(5)	45(5)
C(2)	3938(10)	−2155(14)	979(6)	51(5)
C(3)	4714(11)	−1171(14)	1176(5)	48(5)
C(4)	3947(10)	4219(15)	406(5)	48(5)
C(5)	2920(9)	4733(14)	508(5)	47(5)
C(6)	2108(10)	3746(14)	340(5)	47(5)
N(1′)	6935(8)	3956(11)	2965(4)	48(4)
N(2′)	5910(10)	3909(12)	3954(4)	54(4)
N(3′)	4919(8)	2767(11)	2993(4)	44(4)
N(4′)	5170(8)	5373(11)	2497(4)	40(4)
N(5′)	6215(8)	6508(11)	3419(4)	45(4)
C(1′)	5974(14)	2364(22)	4063(6)	79(8)
C(2′)	5201(15)	1526(16)	3801(7)	74(7)
C(3′)	5261(12)	1460(16)	3235(6)	64(6)
C(4′)	4898(10)	6831(15)	2420(5)	49(5)
C(5′)	5708(12)	7824(16)	2639(6)	58(6)
C(6′)	5788(10)	7825(14)	3204(6)	53(5)
N(6)	6215(8)	1476(13)	1893(4)	49(4)
O(1)	7879(12)	−72(18)	4035(5)	130(8)
O(2)	8030(11)	−162(21)	3180(5)	134(8)
O(3)	9425(8)	128(17)	3674(5)	109(7)
O(4)	8213(10)	1855(14)	3562(7)	124(8)
O(5)	−1598(8)	1373(15)	393(5)	93(6)
O(6)	61(15)	1581(22)	298(11)	209(14)
O(7)	−1012(12)	2551(25)	−228(6)	172(10)
O(8)	−602(25)	3155(36)	549(10)	267(20)
O(9)	1744(8)	3924(13)	1708(4)	76(5)
O(10)	1867(13)	4518(18)	2544(4)	130(8)
O(11)	3288(9)	4146(17)	2094(7)	136(8)
O(12)	2344(11)	6072(13)	1980(7)	128(8)
O(13)	6447(8)	954(13)	1496(4)	73(4)
O(14)	6813(7)	1552(12)	2267(4)	63(4)
O(15)	5335(7)	1981(13)	1917(4)	72(4)
O(16)	6277(7)	2509(13)	394(4)	77(5)

[a] Estimated standard deviations are given in parentheses. Coordinates × 10^n where *n* = 5, 4, 4, 4 for P, O, N, C. Temperature parameters × 10^n where *n* = 4, 3, 3, 3 for P, O, N, C. U_{eq} = the equivalent isotropic temperature parameter. $U_{eq} = {}^1/_2\Sigma_i\Sigma jU_{ij}a_i{}^*a_j{}^*(a_i{\cdot}a_j)$. Primed values indicate that U_{iso} is given. $T = \exp(8\pi^2U_{iso}(\sin^2\theta)/\lambda^2)$.

larger uncertainties than is desirable, but reveal no unusual or unexpected features.

Thermal Stability of *trans*-$CrCl(NH_3)(tn)_2{}^{2+}$. An acidic aqueous solution, pH = 3.0, of the title compound was allowed to stand for several hours in the dark at 28 °C. No proton uptake resulting from loss of ammonia or tn occurred, but a small amount of chloride was aquated. On the basis of a 4-h run and semiquantitative turbidimetric estimation of the released chloride, the rate constant for thermal loss of Cl^- was assigned an upper limit of 5×10^{-7} s^{-1}. This is significantly smaller than the value 9.7×10^{-6} s^{-1} measured for chloride loss from $CrCl(NH_3)_5{}^{2+}$ but is consistent with the values reported earlier for chloropentakis(alkylamino) complexes.[20] The results showed that the compound was sufficiently stable that no corrections for thermal reactions of the starting material were required on the time scale of the photochemical study.

For this study, it was also necessary to explore the thermal stability of the complex in the presence of high concentrations of thiocyanate. We found that two hours dark reaction of the title complex with 3 M NaSCN at 28 °C showed no new HPLC peaks on subsequent analysis.

Table III. Bond Distances (Å) and Angles (deg)[a]

Interatomic Distances			
Cl(1)–Cr(1)	2.317(3)	Cl(1′)–Cr(1′)	2.310(4)
N(1)–Cr(1)	2.089(9)	N(1′)–Cr(1′)	2.106(11)
N(2)–Cr(1)	2.096(10)	N(2′)–Cr(1′)	2.113(11)
N(3)–Cr(1)	2.075(10)	N(3′)–Cr(1′)	2.101(11)
N(4)–Cr(1)	2.079(11)	N(4′)–Cr(1′)	2.079(10)
N(5)–Cr(1)	2.109(10)	N(5′)–Cr(1′)	2.075(11)
C(1)–N(2)	1.494(17)	C(1′)–N(2′)	1.535(25)
C(3)–N(3)	1.554(17)	C(3′)–N(3′)	1.488(19)
C(4)–N(4)	1.523(17)	C(4′)–N(4′)	1.480(18)
C(6)–N(5)	1.524(17)	C(6′)–N(5′)	1.508(18)
C(2)–C(1)	1.534(20)	C(2′)–C(1′)	1.472(26)
C(3)–C(2)	1.496(19)	C(3′)–C(2′)	1.510(24)
C(5)–C(4)	1.515(19)	C(5′)–C(4′)	1.552(21)
C(6)–C(5)	1.510(19)	C(6′)–C(5′)	1.495(22)
Bond Angles			
N(1)–Cr(1)–Cl(1)	179.0(3)	N(1′)–Cr(1′)–Cl(1′)	179.3(3)
N(2)–Cr(1)–Cl(1)	88.2(3)	N(2′)–Cr(1′)–Cl(1′)	88.6(4)
N(2)–Cr(1)–N(1)	90.8(4)	N(2′)–Cr(1′)–N(1′)	91.8(5)
N(3)–Cr(1)–Cl(1)	89.7(3)	N(3′)–Cr(1′)–Cl(1′)	89.8(3)
N(3)–Cr(1)–N(1)	90.0(4)	N(3′)–Cr(1′)–N(1′)	89.6(4)
N(3)–Cr(1)–N(2)	90.6(4)	N(3′)–Cr(1′)–N(2′)	91.9(4)
N(4)–Cr(1)–Cl(1)	90.9(3)	N(4′)–Cr(1′)–Cl(1′)	89.1(3)
N(4)–Cr(1)–N(1)	90.0(4)	N(4′)–Cr(1′)–N(1′)	90.4(4)
N(4)–Cr(1)–N(2)	177.5(4)	N(4′)–Cr(1′)–N(2′)	177.6(5)
N(4)–Cr(1)–N(3)	87.0(4)	N(4′)–Cr(1′)–N(3′)	87.4(4)
N(5)–Cr(1)–Cl(1)	92.3(3)	N(5′)–Cr(1′)–Cl(1′)	90.7(3)
N(5)–Cr(1)–N(1)	88.0(4)	N(5′)–Cr(1′)–N(1′)	89.8(4)
N(5)–Cr(1)–N(2)	90.2(4)	N(5′)–Cr(1′)–N(2′)	89.3(4)
N(5)–Cr(1)–N(3)	177.8(4)	N(5′)–Cr(1′)–N(3′)	178.7(4)
N(5)–Cr(1)–N(4)	92.2(4)	N(5′)–Cr(1′)–N(4′)	91.4(4)
C(1)–N(2)–Cr(1)	121.0(8)	C(1′)–N(2′)–Cr(1′)	121.0(8)
C(3)–N(3)–Cr(1)	120.3(8)	C(3′)–N(3′)–Cr(1′)	120.6(9)
C(4)–N(4)–Cr(1)	118.0(8)	C(4′)–N(4′)–Cr(1′)	120.4(8)
C(6)–N(5)–Cr(1)	117.9(8)	C(6′)–N(5′)–Cr(1′)	120.0(8)
C(2)–C(1)–N(2)	111.2(11)	C(2′)–C(1′)–N(2′)	115.1(14)
C(3)–C(2)–C(1)	114.4(12)	C(3′)–C(2′)–C(1′)	114.8(15)
C(2)–C(3)–N(3)	111.2(11)	C(2′)–C(3′)–N(3′)	111.1(13)
C(5)–C(4)–N(4)	113.1(11)	C(5′)–C(4′)–N(4′)	112.5(11)
C(6)–C(5)–C(4)	113.2(11)	C(6′)–C(5′)–C(4′)	112.9(12)
C(5)–C(6)–N(5)	113.4(10)	C(5′)–C(6′)–N(5′)	112.6(12)

[a] Estimated standard deviations are given in parentheses.

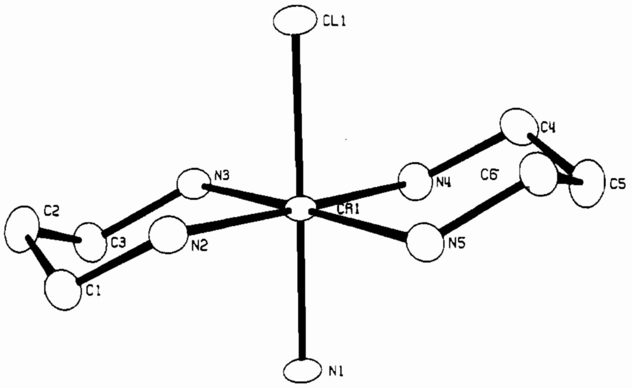

Figure 1. ORTEP diagram of *trans*-$CrCl(NH_3)(tn)_2{}^{2+}$.

Photoaquation and Photoanation. Photolysis of the compound at pH 3.0 in either of the ligand field absorption bands led to efficient proton uptake with a quantum yield of 0.32 at 28 °C. At the same time, total chloride release both during and after the photolysis period was below the level of detection, corresponding to an upper limit for the quantum yield of chloride loss of 0.003. These features were reassuring. Previous work on other systems has shown[20,24] that it is possible for thermal halide aquation from the main haloaquo photoproduct to be far more significant than thermal or photochemical halide loss from the starting material. This was not a problem in the present system.

---

(24) Kirk, A. D.; Arunachalam, S.; Kneeland, D. *Inorg. Chem.* **1986**, *25*, 3552.

Table IV. Quantum Yields of Proton Uptake[a]

condition	360 nm, 28 °C	436 nm, 28 °C	436 nm, 10 °C
in the absence of NaSCN	0.325 (4)	0.324 (2)	0.335 (2)
in the presence of NaSCN[b]	0.300 (2)	0.330 (2)	

[a] Relative standard deviations ±3%. Number of runs given in parentheses. [b] There was no variation of proton uptake quantum yield in the range 1–3 M NaSCN.

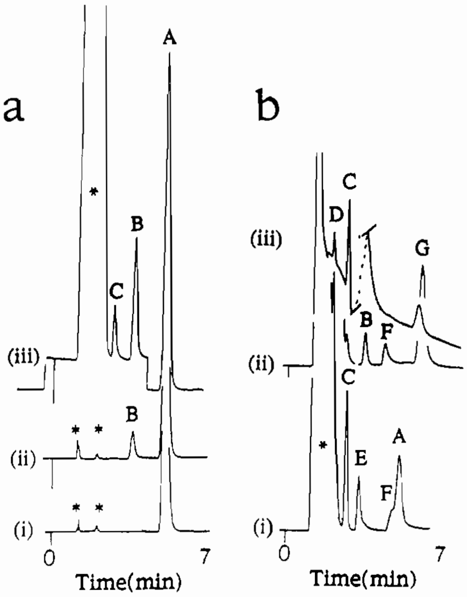

Figure 2. HPLC identification of products. (a) (i) Starting complex: *trans*-$CrCl(NH_3)(tn)_2^{2+}$. (ii) Photoaquation of *trans*-$CrCl(NH_3)(tn)_2^{2+}$. (iii) Photoanation of *trans*-$CrCl(NH_3)(tn)_2^{2+}$ with 3 M NCS^-. (b) (i) Thermal aquation of *trans*-$CrCl_2(tn)_2^+$ and subsequent thermal anation with NCS^-; spiked with *trans*-$CrCl(NH_3)(tn)_2^{2+}$. (ii) Thermal aquation of *cis*-$CrCl_2(tn)_2^+$ and subsequent thermal anation with NCS^-. (iii) Photoaquation of *trans*-$CrCl_2(tn)_2^+$ and subsequent thermal anation with NCS^-. (To get this chromatogram on the figure scale it was necessary to cut in the region where B and E elute. There were no significant peaks in this region.) Key: peak label (elution time, min), identity, A (5.1), *trans*-$CrCl(NH_3)(tn)_2^{2+}$; B (3.6), *cis*-$CrCl(H2O)(tn)_2^{2+}$; C (2.6), *cis*-$CrCl(NCS)(tn)_2^+$; D (1.96), *trans*-$CrCl_2(tn)_2^+$; E (3.2), *trans*-$CrCl(NCS)(tn)_2^+$; F (4.7), *trans*-$CrCl(H_2O)(tn)_2^{2+}$; G (5.8), *cis*-$Cr(NCS)(H_2O)(tn)_2^{2+}$. The large peak marked with an asterisk is due to the NCS^- ion; the small ones are impurity peaks.

Photolysis in the presence of 1–3 M thiocyanate and pH 3.0 also led to proton uptake *at the same rate as in its absence.* Table IV summarizes the quantum yields of proton uptake measured with and without added thiocyanate up to 3 M at irradiation wavelengths of 360 and 436 nm.

Chromatographic Identification of Photoproducts. Products were identified by HPLC chromatographic retention times of the title compound and of thermalized and/or photolyzed solutions of *trans*- or *cis*-$CrCl_2(tn)_2^+$ as follows. Separate thermolyses of *trans*- and *cis*-$CrCl_2(tn)_2^+$ and chromatographic analyses (not shown) established the elution times and peak characteristics for these starting compounds and their stereoretained chloroaquobisdiaminopropane products. In both pairs, the *cis* isomer eluted before the *trans* (1.88 and 1.96 min respectively for the dichloro species) with the aquochloro isomers giving broader peaks at longer retention times (3.6 and 4.7 min, B and F respectively in Figure 2).

The chromatogram of the starting material Figure 2a(i) revealed two small impurity peaks marked with asterisks (they correspond to less than 1% of the area of the main peak). After photoaquation of *trans*-$CrCl(NH_3)(tn)_2^{2+}$ (A), chromatographic analysis gave the result shown in Figure 2a(ii). The single resolved photoaquation product B had the same retention time (3.6 min) as *cis*-$CrCl(H_2O)(tn)_2^{2+}$ prepared in solution (and checked by UV–vis spectroscopy) by thermal aquation of *cis*-$CrCl_2(tn)_2^+$, Figure 2b(ii), or by photoaquation of *trans*-$CrCl_2(tn)_2^+$ (peak B is not seen in Figure 2b(iii) because of the cutting neeeded to present this chromatogram on scale, but it appears as a shoulder on the side of the large thiocyanate peak in the original chromatogram). No *trans*-aquochloro product was observed.

Photolysis in the presence of NCS^-, Figure 2a(iii), led to an additional product, C, with a retention time of 2.6 min, about the value expected for a singly charged ion of type $CrXY(tn)_2^+$. It was established to be *cis*-$CrCl(NCS)(tn)_2^+$, by a series of experiments, initially based on the assumption of stereoretentive aquation followed by anation, but later recognising the real complexities of the systems.

trans-$CrCl_2(tn)_2^+$ was aquated at 40 °C followed by addition of 1 M NCS^- ion and subsequent thermal anation at 50 °C. Many experiments were carried out at different times and conversions and only the result for extensive conversion is shown here, as Figure 2b(i). Peak F is the initial product of aquation, *trans*-$CrCl(H_2O)(tn)_2^{2+}$, while peak A is title compound deliberately added in this run to prove that it was resolved from the other product peaks. Peaks C and E (note that E and B are *not* coincident peaks) are the isomers of $CrCl(NCS)(tn)_2^+$. The problem was to assign the sequence, and to clarify the following discussion we state here that we concluded it is C = *cis* and E = *trans*. This was surprising and confusing since the stereoretained *trans* product then has to be the smaller peak.

This conclusion was reached by comparison of these results with further thiocyanate anation experiments that began with solutions containing *cis*-$CrCl(H_2O)(tn)_2^+$ obtained by two routes. In the first, *cis*-$CrCl_2(tn)_2^{2+}$ was almost completely thermolyzed to produce the aquo product, as decided by comparison of the UV–vis spectrum with our expectations for the aquo product, and then anated with thiocyanate. In the chromatogram of this solution, Figure 2b(ii), a small peak for C is seen, along with unchanged *cis*-$CrCl(H_2O)(tn)_2^{2+}$, B. Peak E is completely absent. This is the basis on which we assign peak C to the *cis* isomer of $CrCl(NCS)(tn)_2^+$. It is not the major product of the reaction, however. This is *cis*-$Cr(NCS)(H_2O)(tn)_2^{2+}$ which is found as a peak, G, at 5.8 min. As a complicating factor in the high conversion chromatogram shown in the figure, there is also some *trans*-$CrCl(H_2O)(tn)_2^{2+}$, F. This likely arose by isomerization of the *cis*-aquochloro isomer, as it was absent in a chromatogram of the same solution at an earlier stage of thermalization.

The results for the second route are less complex and confirm the above assignment. Figure 2b(iii) shows the result of thermal thiocyanate anation of a solution of *trans*-$CrCl_2(tn)_2^+$ first partially photolyzed to generate *cis*-$CrCl(H_2O)(tn)_2^{2+}$. The preponderance of peaks C and G among the products is evident, along with the cleaner nature of the reactions. This is understandable in terms of the greater thermal stabilities of the complexes of the *trans* series and the selective character of the photochemical generation of *cis*-$CrCl(H_2O)(tn)_2^{2+}$.

It is interesting that the main product of the reaction between thiocyanate and *cis*-$CrCl(H_2O)(tn)_2^{2+}$ is not the anation product, C, but peak G, *cis*-$Cr(NCS)(H_2O)(tn)_2^{2+}$. This product does not appear in the experiments starting with *trans*-$CrCl(H_2O)(tn)_2^{2+}$ which give mainly *cis*-$CrCl(NCS)(tn)_2^+$, Figure 2b(i). It must therefore be the result not of anation followed by chloride aquation from *cis*-$CrCl(NCS)(tn)_2^+$ but of direct displacement by thiocyanate of chloride from *cis*-$CrCl(H_2O)(tn)_2^{2+}$. This stimulated us to seek the same process in the *trans* series; in a further series of experiments starting with *trans*-$CrCl_2(tn)_2^+$, a small broad peak was found at about 10-min elution time with the characteristics expected for *trans*-$Cr(NCS)(H_2O)(tn)_2^{2+}$. Both isomers of the aquochloro complex therefore exhibit this direct chloride displacement reaction.

Despite their unusual features, the results establish the complete peak sequence for these complexes. They are all resolved, and in all cases the *cis* isomer elutes before its corresponding *trans* isomer. This is opposite to the sequence observed in conventional ion-exchange separations but this is understandable given the inverted polarity characteristics of the reversed-phase HPLC technique.

Although our product analysis results do not establish whether the isomerisation processes observed are associated with the aquation or anation steps of the thermal reactions, the results indicate that the following kinetic scheme applies:

$$\textit{trans}\text{-CrCl}_2(\text{tn})_2{}^+ \xrightarrow[\text{aquation and anation}]{} \textit{trans}\text{-Cr(NCS)(H}_2\text{O)(tn)}_2{}^{2+}\text{(minor)}$$

$$\rightarrow \textit{trans}\text{-CrCl(NCS)(tn)}_2{}^+\text{ (minor)}$$

$$\rightarrow \textit{cis}\text{-CrCl(NCS)(tn)}_2{}^+\text{ (major)}$$

$$\textit{cis}\text{-CrCl}_2(\text{tn})_2{}^+ \xrightarrow[\text{aquation and anation}]{} \textit{cis}\text{-Cr(NCS)(H}_2\text{O)(tn)}_2{}^{2+}\text{ (major)}$$

$$\rightarrow \textit{cis}\text{-CrCl(NCS)(tn)}_2{}^+\text{ (minor)}$$

The further exploration of this interesting thermal behavior was left for future work.

To investigate whether any photoproduct of *trans*-$CrCl(NH_3)(tn)_2^{2+}$ with monodentate protonated tn (ie. 3+ products) had formed, chromatograms were recorded under different eluent conditions thought to be more appropriate for 3+ ions (25 mM BSA/TEA in 100% H_2O, pH 3.1). The retention times of $Cr(tn)_3^{3+}$ and *cis*-$Cr(NH_3)_2(tn)_2^{3+}$, used as models for the possible tn-loss photoproducts, were found to be 13.3 and 12.1 min, respectively. Photolyzed solutions (436 nm, 28 °C) of *trans*-$CrCl(NH_3)(tn)_2^{2+}$ showed only two peaks at 14.1 and 5.5 min corresponding to *trans*-$CrCl(NH_3)(tn)_2^{2+}$ and *cis*-$CrCl(H_2O)(tn)_2^{2+}$, respectively. Despite the surprisingly long retention time for the starting material under these conditions,[25] no other peaks were observed for possible 3+ photoproducts.

Spectroscopic Identification of Anation Photoproduct. A photolysed solution of *trans*-$CrCl(NH_3)(tn)_2^{2+}$ was loaded on to a Sephadex cation-exchange column. The first photoproduct was eluted with 0.02 M sodium perchlorate solution as would be expected for a singly charged cation. The UV–vis spectrum of the eluent showed two broad absorption bands with wavelength maxima at about 380 and 500 nm and an absorbance ratio in the range 1.2 to 1.3. The spectrum of the analogue *cis*-$CrCl(NCS)en_2^+$ has[26] the following λ_{max} (ϵ) values: 385 (71) and 506 (91) nm. In contrast the *trans* isomer has[27] bands at 380 (56) and 530 (50) nm, with a weak third component at 450 (25) nm. The wavelength of the first ligand field band and the ϵ_1/ϵ_2 ratio of the bands both support the assignment of the photoanation product as *cis*-$CrCl(NCS)(tn)_2^+$.

Discussion

Molecular Structure. The analytical and UV–vis spectroscopic data established the compound to be $[CrCl(NH_3)(tn)_2](ClO_4)_2$, and the chromatographic results showed that any impurities either were not separated from the title compound or were less than 1%. The X-ray crystal structure determination demonstrated unequivocally that the complex under study was the *trans* isomer. This proof is, of course, crucial to our analysis of the stereochemistry of photoaquation and anation. The structure of the ion is extremely similar to that reported already for the analogous fluoro compound,[22] and in particular, the arrangement of the chair form tn rings is identical in the two systems. The structure presents no unusual features.

Basic Photochemistry. The data from proton uptake and HPLC show that for irradiation at both 360 and 436 nm, the dominant photochemical process is substitution of the NH_3 ligand with a temperature-independent quantum yield of 0.33. This yield is the same as that for the analogous en complex.[9] As a further parallel, the substituting water ligand enters trans to the displaced ammonia ligand, yielding *cis*-$CrCl(H_2O)(tn)_2^{2+}$. No *trans* product was observed; this places an approximate limit of greater than 95% cis on the product isomer yield. The yields of any other reaction modes were small so the molecule has a single dominant photolysis mode.

The results are consistent with other observations of photoaquation of an axial ligand in a C_{4v} or D_{4h} complex and also with both an angular overlap model of d^3 photostereochemistry and more recent ab initio theory.[28] Indeed, the molecule was deliberately chosen in anticipation of this single uncomplicated photoaquation mode, loss of the trans ammonia with stereochemical change. The expectation follows from theory and parallels to other results, coupled with the demonstrated poor leaving ligand ability of the tn ligand;[19] this serves to minimize the competing process involving loss of the equatorial ligands such as occurs in the ethylenediamine analogues.

What was of more interest here, however, is that all the processes stereochemically studied to date have been photosolvations, and the large majority of these, photoaquations. We sought in this study to extend the data base to other types of substitution process.

Photoanation Processes. Wasgestian[11,12] and co-workers have found that photoanation of $Cr(NH_3)_6^{3+}$ occurs in concentrated solutions of chloride and thiocyanate. The question immediately arises as to whether such a substitution process involving a negatively charged entering group should also occur with stereochemical change. We considered that a study of the thiocyanate anation of the title compound would offer the best chance of an unambiguous answer.

The quantum yield data of Table IV and the chromatographic study of the photoproducts shown in summary form in Figure 2 show that thiocyanate photoanation of *trans*-$CrCl(NH_3)(tn)_2^{2+}$ competes effectively with photoaquation and produces *cis*-$CrCl(NCS)(tn)_2^+$ as the only major photoanation product. We observe qualitatively that an increase of NCS^- concentration increased the formation of *cis*-$CrCl(NCS)(tn)_2^+$ and decreased *cis*-$CrCl(H_2O)(tn)_2^{2+}$. This is consistent with the quantum yield data that demonstrate the same proton uptake quantum yield with and without thiocyanate present. Wasgestian and co-workers[11,12] also unambiguously demonstrated that the two modes of reaction were in competition in their systems.

Our results showed that the anation product arose exclusively by the photoprocess and not by thermal anation of photoproducts. This finding is fortified by our observation that the dominant dark reaction between thiocyanate and *cis*-$CrCl(H_2O)(tn)_2^{2+}$ at the higher temperature of 50 °C is direct chloride substitution to give *cis*-$Cr(NCS)(H_2O)(tn)_2^{2+}$ with only a minor contribution of anation to *cis*-$CrCl(NCS)(tn)_2^+$. Given the very high thiocyanate concentrations used, it is likely that the photoactive species is a complex/thiocyanate ion pair.

The work shows that thiocyanate anation occurs along the same stereochemical pathway as the photoaquation process.

Commentary. The exact nature of this pathway is still a subject of discussion, but in our view,[7] the route most consistent with photophysical and photochemical evidence is an associative reaction of the excited quartet state. Alternative models involving

---

(25) The variations of retention time with conditions in ion-interaction, reversed-phase HPLC are not perfectly understood.

(26) Garner, C. S.; House, D. A. *Transition Met. Chem.* (*N.Y.*) **1970**, *6*, 59.

(27) Gandolfi, M. T.; Manfrin, M. F.; Moggi, L.; Balzani, V. *J. Am. Chem. Soc.* **1972**, *94*, 7152.

(28) Vanquickenborne, L. G.; Coussens, B.; Ceulemans, A.; Pierloot, K. *Inorg. Chem.* **1992**, *31*, 539.

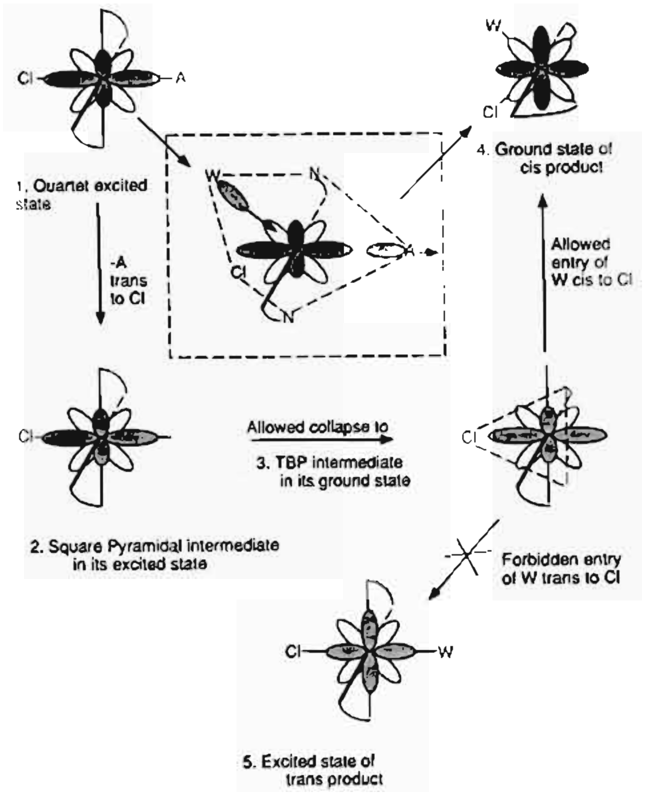

Figure 3. Mechanism of photoaquation and photoanation of *trans*-CrCl(NH_3)(tn)$_2^{2+}$. The course of photosubstitution can be followed based on the proposed reaction via a trigonal-bipyramidal intermediate.[28] The first step shows the outcome of electronic excitation. Rotation of charge on to the metal ligand bond axes leads to one component of the lowest excited ^4E_g state of the complex, species 1. Here the excitation plane has been chosen to be the plane of the paper, and all subsequent ligand motions shown occur in this plane. Because of the presence of the weak field chloride ligand, the sigma antibonding orbital populated has increased d_{z^2} character, and the ammonia trans to chloride is preferentially dissociated, leading to a square-pyramidal (SP) intermediate, species 2. This can rearrange in an allowed process to a lower energy trigonal-bipyramidal intermediate (TBP), species 3, having chloride in the equatorial position and, for this system, in its ground electronic state. Subsequent solvent attack on this TBP intermediate at the two edges cis to chloride may then follow by an allowed process leading to the ground state of *cis*-CrCl(H_2O)(tn)$_2^{2+}$, species 4. In contrast, entry of solvent trans to chloride would lead to the electronically excited state of the *trans* product, species 5, and is therefore forbidden. The boxed inset shows an equivalent seven-coordinate process occuring via an asymmetric pentagonal-bipyramidal intermediate having long bonds to the entering and leaving ligands. Such an interchange intermediate is suggested by the negative volumes of activation found for Cr(III) photosubstitution.[32]

the doublet state[29] or a ground-state intermediate[30] do not apparently provide any rationale for the observed stereochemical change.

Such a pathway can be based either on published theoretical models involving five-coordinate intermediates[3,28] or, at least in principle, the same concepts modified to recognize the seven-coordinate character of the transition state.[7] This latter seems to be required by the negative volumes of activation observed for the photoaquation reactions of these cationic complexes.[31,32] The most reasonable geometric configuration for the seven coordinate intermediate is an asymmetric pentagonal bipyramidal (pbp) species in which the Cr center has long bonds to the entering and leaving ligands.

To clarify this brief description, a representation of the reaction pathway and the distinction between the two putative intermediates is shown in Figure 3. The published theoretical models propose the pathway via square-pyramidal and trigonal-bipyramidal five-coordinate intermediates shown pictorially in the main part of the diagram. Restrictions on the allowed rearrangements and positions of entry of a nucleophile lead in a symmetry-allowed fashion to the stereochemically changed product. The central inset in the figure shows how an analogous process could be imagined to occur via the asymmetric pentagonal-bipyramidal intermediate, satisfying the volume of activation evidence. The only real difference would be the exact sequence of bond breaking and formation; the symmetry requirements could be essentially unchanged.

This study has shown that, whatever the details of this pathway, it is not changed, at least in this instance, by altering the charge on the entering nucleophile.

Acknowledgment. The authors wish to thank the Natural Sciences and Engineering Research Council of Canada and the University of Victoria for their financial support of this work. C.N. thanks Bharathiar University for a leave of absence. C. Beveridge kindly obtained the crystallographic data and carried out the structure analysis.

Supplementary Material Available: Complete tables (Tables S1–S5) with full crystal data and collection parameters, bond lengths and angles, non-bonded distances and anisotropic temperature parameters (10 pages). Ordering information is given on any current masthead page.

---

(29) Forster, L. S. *Chem. Rev.* **1990**, *90*, 331.

(30) Endicott, J. F.; Ramasami, T.; Tamilarasan, R.; Lessard, R. B.; Brubaker, G. R. *Coord. Chem. Rev.* **1987**, *77*, 1.

(31) Angermann, K.; van Eldik, R.; Kelm, H.; Wasgestian, F. *Inorg. Chem.* **1981**, *20*, 955.

(32) Vincze, L.; Friesen, D. A.; Mezyk, S. P.; Waltz, W. L. *Inorg. Chem.* **1992**, *31*, 4950.